Marchenko wavefield redatuming, imaging conditions, and the effect of model errors

de Ridder, Sjoerd; van der Neut, Joost; Curtis, A; Wapenaar, Kees

Important note
To cite this publication, please use the final published version (if applicable).
Please check the document version above.

Marchenko wavefield redatuming, imaging conditions, and the effect of model errors

Sjoerd de Ridder*, University of Edinburgh; Joost van de Neut, Delft University of Technology; Andrew Curtis, University of Edinburgh; Kees Wapenaar, Delft University of Technology

SUMMARY

Recently, a novel method to redatum the wavefield in the subsurface from a reflection response measured at the surface has gained interest for imaging primaries in the presence of strong internal multiples. A prerequisite for the algorithm is an accurate and correct estimate of the direct-wave Green's function. However, usually we use an estimate for the direct-wave Green's function computed in a background velocity medium. Here, we investigate the effect of amplitude and phase errors in that estimate. We formulate two novel imaging conditions based on double-focusing the measured reflection response inside the subsurface. These yield information on the amplitude error in the estimate for the direct-wave Green's function which we can then correct, but the phase error remains elusive.

INTRODUCTION

Machenko wavefield redatuming (MWR) refers to redatuming a wavefield, recorded as reflection response outside a stack of layers to transmission responses inside the stack of layers using the inverse of the direct wave, by solving the Marchenko equations for a set of focusing functions (Broggini et al., 2012; Wapenaar et al., 2014). In MWR, redatuming strictly means to emulate a recording as if it was recorded at a traveltime (not at a specific known physical location) inside the subsurface. Because the redatumed wavefield does not suffer from spurious waves (such as primaries and internal multiples, reverse-time propagated beyond their originator interfaces), therefore this technique allows for artifact free imaging of primaries.

Several imaging schemes have been proposed. MWR can be applied at each depth level followed by a deconvolution of upgoing with downgoing waves (Broggini et al., 2014; Wapenaar et al., 2014) or cross-correlation (Behura et al., 2014). Slob et al. (2014) proposed to extract the image at the one-way travel-time of the direct wave directly from the retrieved upgoing focusing function.

Although the scheme proves relatively stable against velocity errors (Thorbecke et al., 2013), accurate Green's function (GF) extrapolation relies on an accurate model of the direct wave Green's function (DWGF). We investigate the effect of a general amplitude and phase error in an estimated DWGF.

Wapenaar et al. (2016) derived expressions to redatum two-way GFs from single-sided illumination, yielding both virtual sources and virtual receivers inside the subsurface. We follow a similar derivation, starting from one-way reciprocity theorems to derive two new imaging conditions. The first images the scattered wavefield, while the second images the virtual source strength for virtual sources focused throughout the medium. Finally, we investigate how amplitude and phase errors in the estimated DWGF appear in images, and show how the amplitude error can be corrected.

MARCHENKO WAVEFIELD REDATUMING

The basis for 1D MWR lies in the Marchenko equations (Wapenaar et al., 2014) that relate the transmission GFs from the acquisition level at z_1 (on top of a layer-stack) to z_2 within the layer-stack, with the reflection response measured at the aquisition level and focusing functions (FFs) that form a focusing wavefield at z_2. A GF measured at z_r in response to a source at z_s is denoted $G^{-,+}(z_r, z_s)$, where the superscripts indicate respectively upward recording (at z_r) and a downward radiating source (at z_s). The wavefield downward radiated and injected at z_i and focussing at z_f is denoted $f^+(z_i, z_f)$, the resulting back-scattered upward wavefield recorded at z_r is denoted $f^-(z_r, z_f)$. We use a formulation based on flux normalization. The explicit frequency dependence of the GFs and FFs are omitted for notation brevity, and a bar ($^-$) denotes complex conjugation. We have the following reciprocity relations for the flux normalized one-way GFs: $G^{+,+}(z_1, z_2) = -G^{-,-}(z_2, z_1)$ and $G^{+,-}(z_1, z_2) = G^{+,-}(z_2, z_1)$, $G^{-,+}(z_1, z_2) = G^{-,+}(z_2, z_1)$ (Wapenaar and Grimbergen, 1996). In the frequency domain these can be written:

$$-G^{-,+}(z_2, z_1) = f^-(z_1, z_2) - G^{-,+}(z_1, z_1)f^+(z_1, z_2),, \quad (1)$$

$$\overline{G}^{+,+}(z_2, z_1) = f^+(z_1, z_2) - \overline{G}^{-,+}(z_1, z_1)f^-(z_1, z_2)., \quad (2)$$

These two equations have four unknowns and only one known (the recorded reflection data $G^{-,+}(z_1, z_1)$). We reduce the rank of the system by imposing a causality condition for the Green's and focusing functions. A frequency-domain operator Θ applies what amounts to a mute function in the time-domain. We suppress all energy in a trace that arrives at the same time or after the direct wave (symmetrically in time). Thus, $\Theta\{G^{-,+}(z_2, z_1)\} = 0$ and $\Theta\{\overline{G}^{+,+}(z_2, z_1)\} = 0$. We further reduce the degeneracy of the system by splitting the downgoing FF in a direct wave focussing function (DWFF) and a coda, $f^+(z_1, z_2) = f_d^+(z_1, z_2) + f_m^+(z_1, z_2)$. The DWFF equals the inverse of the DWGF. The muting function applied to the downgoing FF suppresses the DWFF but leaves the coda, $\Theta\{f^+(z_1, z_2)\} = f_m^+(z_1, z_2)$. Applying the muting operator to Equations 1 and 2 leaves us with two equations and only three unknowns:

$$f^-(z_1, z_2) = \Theta\{G^{-,+}(z_1, z_1) \left[f_d^+(z_1, z_2) + f_m^+(z_1, z_2)\right]\}, \quad (3)$$

$$f_m^+(z_1, z_2) = \Theta\{\overline{G}^{-,+}(z_1, z_1)f^-(z_1, z_2)\}. \quad (4)$$

One way to solve these equations is by iterating between Equations 3 and 4 starting with the true f_d^+, $f_m^+ = 0$, and $f^- = 0$ (van der Neut et al., 2015). The retrieved FFs are then employed to find the full GFs between a point in the subsurface, z_2, and the surface, z_1, using Equations 1 and 2. We can repeat this procedure and retrieve the wavefield at all points in the subsurface (Broggini et al., 2014). This amounts to extrapolation of our surface data to the subsurface as though

we recorded a vertical-seismic profile. This interpretation is only valid in the absence of model errors. Figure 1 shows an example in a three layer medium, using the true model to compute a DWFF and extrapolate the measured reflection response into the subsurface. The medium consists of two interfaces 100 m apart, forming a layer-sandwich with respectively $v_1 = 1500 \; m/s$, $v_2 = 2000 \; m/s$, $v_3 = 2500 \; m/s$, and constant density of $\rho_1 = \rho_2 = \rho_3 = 2000 \; kg/m^3$. We did not include the free surface in the formulations in this study, but the Marchenko scheme can be extended to include the free surface (Singh et al., 2015). The reflection coefficients for downgoing wavefields are $\frac{\rho_2 v_2 - \rho_1 v_1}{\rho_2 v_2 + \rho_1 v_1} \approx 0.143$ and $\frac{\rho_3 v_3 - \rho_2 v_2}{\rho_3 v_3 + \rho_2 v_2} \approx 0.111$ at respectively the first and second interface from the top, and for upgoing wavefields respectively ~ -0.143 and ~ -0.111.

Generally we will use a model estimate to compute an estimated DWGF and DWFF. These estimates, denoted with a tilde ($\tilde{}$), relate to the unknown true functions subject to an error in amplitude, α, and phase, $\omega\beta$:

$$\widetilde{G}_d^{+,+}(z_2,z_1) = \alpha^{-1}(z_1,z_2)\exp\{-i\omega\beta(z_1,z_2)\} \, G_d^{+,+}(z_2,z_1),$$

$$\widetilde{f}_d^{+}(z_1,z_2) = \alpha(z_1,z_2)\exp\{i\omega\beta(z_1,z_2)\} \, f_d^{+}(z_1,z_2). \quad (5)$$

The amplitude $\alpha(\omega)$ and phase errors $\beta(\omega)$, can be a function of frequency, i.e. a dispersive velocity error. Here, the amplitude and phase errors on the DWGF and DWFF are mutually consistent. It is the DWFF in Equation 5 that is input into the iterative scheme based on Equations 3 and 4. We retrieve the full FFs subject to the following errors in amplitude and phase:

$$\widetilde{f}^{+}(z_1,z_2) = \alpha(z_1,z_2)\exp\{i\omega\beta(z_1,z_2)\} \, f^{+}(z_1,z_2), \quad (6)$$

$$\widetilde{f}^{-}(z_1,z_2) = \alpha(z_1,z_2)\exp\{i\omega\beta(z_1,z_2)\} \, f^{-}(z_1,z_2). \quad (7)$$

When we employ these FFs to extrapolate the surface recorded GFs using the Marchenko Equations 1 and 2, we retrieve:

$$\widetilde{G}^{-,+}(z_2,z_1) = \alpha(z_1,z_2)\exp\{\; i\omega\beta(z_1,z_2)\} \, G^{-,+}(z_2,z_1), \quad (8)$$

$$\widetilde{G}^{+,+}(z_2,z_1) = \alpha(z_1,z_2)\exp\{-i\omega\beta(z_1,z_2)\} \, G^{+,+}(z_2,z_1). \quad (9)$$

Notice that the amplitude error on the retrieved GF is inverted with respect to the amplitude error on the estimated GF of Equation 5. The phase-errors in the retrieved GFs of up- and downgoing wavefields act in opposite directions.

Figure 2 shows an example of the effect of amplitude and phase errors in the estimated DWFF. The input reflection-data are the same as for the example in Figure 1, but the DWFF was computed in a homogeneous background velocity. The retrieved full FFs and the retrieved wavefield in the subsurface are shifted in time. We redatumed a wavefield in the subsurface with amplitude and kinematics derived from the estimate of the DWFF, but with the structure (in terms of primaries and multiples) of that of the true medium. This example showcases the strength of Marchenko wavefield redatuming: an image, defined for example by deconvolution of up and downgoing wavefields, will be clean of spurious reflectors (Broggini et al., 2014; Wapenaar et al., 2014).

IMAGING CONDITIONS

Classical scattering-type imaging conditions are based on establising a causal condition between a source wavefield and a

recorded wavefield (Claerbout, 1985). The source and recorded receiver wavefields are extrapolated (or respectively forward and reverse-time propagated) back into the subsurface. When both wavefields overlap in time and space, we hypothesize that the source wavefield excited the recorded wavefield through back-scattering (the reflector acting as exploding-reflector or secondary Huygens source). We typically establish a causal condition between the two wavefields by deconvolution or correlation, and extracting the energy at $t = 0$. Similarly, a source-type imaging condition for primary (non-Huygens) sources is defined by extrapolating (or back-propagating) the recorded wavefield and extracting the energy at $t = 0$.

FFs undo propagation of wavefields and therefore MWR provides an alternative avenue of wavefield redatuming into the subsurface (Wapenaar et al., 2016). We exploit this property and derive imaging conditions by applying FFs to GF's. We start with one-way reciprocity relations, between states A and B, of the convolution- and correlation-type in 1D media (Wapenaar, 1996):

$$\left\{ P_A^+ P_B^- - P_A^- P_B^+ \right\}\Big|_{z_2} - \left\{ P_A^+ P_B^- - P_A^- P_B^+ \right\}\Big|_{z_1} = \quad (10)$$

$$\int_{z_1}^{z_2} dz \left\{ P_A^+ S_B^- - P_A^- S_B^+ \right\} + \int_{z_1}^{z_2} dz \left\{ S_A^+ P_B^- - S_A^- P_B^+ \right\},$$

$$\left\{ P_A^+ \overline{P}_B^+ - P_A^- \overline{P}_B^- \right\}\Big|_{z_2} - \left\{ P_A^+ \overline{P}_B^+ - P_A^- \overline{P}_B^- \right\}\Big|_{z_1} = \quad (11)$$

$$\int_{z_1}^{z_2} dz \left\{ P_A^+ \overline{S}_B^+ - P_A^- \overline{S}_B^- \right\} + \int_{z_1}^{z_2} dz \left\{ S_A^+ \overline{P}_B^+ - S_A^- \overline{P}_B^- \right\}.$$

We are interested in deriving relationships between focusing functions emitted from the acquisition surface at $z = z_1$ and focusing at depth level $z = z_2$, and Green's functions recorded at $z = z_1$ of a source at $z = z_2$. The source at $z = z_2$ can either be down- or upward radiating.

We start by considering a downward radiating source at $z = z_2$. The wavefield, boundary conditions, and source states, in states A (a reference medium and truncated below z_2) and B (the actual medium) are given by:

STATE A
At z_1: $P_A^+ = f_1^+(z_1,z_2)$, $P_A^- = f_1^-(z_1,z_2)$
At z_2: $P_A^+ = 1$, $P_A^- = 0$
Wavefields for $z_1 < z < z_2$: $P_A^+ = f_1^+(z,z_2)$, $P_A^- = f_1^-(z,z_2)$
Sources for $z_1 < z$: $S_A^+ = 0$, $S_A^- = 0$
STATE B
At z_1: $P_B^+ = 0$, $P_B^- = G^{-,+}(z_1,z_2)$
At z_2: $P_B^+ = G^{+,+}(z_2,z_2)$, $P_B^- = G^{-,+}(z_2,z_2)$
Wavefields for $z_1 < z < z_2$: $P_A^- = \widetilde{f}_1^-(z,z_2)$, $P_B^- = G^{-,+}(z,z_2)$
Sources for $z_1 < z$: $S_B^+ = \delta(z-z_2)$, $S_B^- = 0$
Substitution of these states into Equations 10 and 11, yields:

$$f^+(z_1,z_2)G^{-,+}(z_1,z_2) = G^{-,+}(z_2,z_2) + \frac{1}{2}f^-(z_2,z_2) \quad (12)$$

$$-f^-(z_1,z_2)\overline{G}^{-,+}(z_1,z_2) = \overline{G}^{+,+}(z_2,z_2) - \frac{1}{2}f^+(z_2,z_2). \quad (13)$$

We can repeat this procedure while considering an upward radiating source at $z = z_2$. The wavefield, boundary conditions, and source states, in states A and B are given by:

Marchenko Imaging Conditions

STATE A

At z_1: $P_A^+ = f_1^+(z_1, z_2)$, $P_A^- = f_1^-(z_1, z_2)$
At z_2: $P_A^+ = 1$, $P_A^- = 0$
Wavefields for $z_1 < z < z_2$: $P_A^+ = f_1^+(z, z_2)$, $P_A^- = f_1^-(z, z_2)$
Sources for $z_1 < z < z$: $S_A^+ = 0$, $S_A^- = 0$

STATE B

At z_1: $P_B^+ = 0$, $P_B^- = G^{-,-}(z_1, z_2)$
At z_2: $P_B^+ = G^{+,-}(z_2, z_2)$, $P_B^- = G^{-,-}(z_2, z_2)$
Wavefields for $z_1 < z$: $P_B^+ = G^{+,-}(z, z_2)$, $P_B^- = G^{-,-}(z, z_2)$
Sources for $S_B^+ = 0$, $S_B^- = \delta(z - z_2)$
Substitution of these states into Equations 10 and 11, yields:

$$f^+(z_1, z_2)G^{-,-}(z_1, z_2) = G^{-,-}(z_2, z_2) - \frac{1}{2}f^+(z_2, z_2) \quad (14)$$

$$-f^-(z_1, z_2)\overline{G}^{-,-}(z_1, z_2) = \overline{G}^{+,-}(z_2, z_2) + \frac{1}{2}f^-(z_2, z_2). \quad (15)$$

Because the reference medium (State A) is homogeneous at and below z_2, we have $f^+(z_2, z_2) = 1$ and $f^-(z_2, z_2) = 0$. Subtracting 14 from 13 yields:

$$-f^+(z_1, z_2)G^{-,-}(z_1, z_2) - f^-(z_1, z_2)\overline{G}^{-,+}(z_1, z_2) = \quad (16)$$
$$\left[\overline{G}^{+,+}(z_2, z_2, \omega) - G^{-,-}(z_2, z_2, \omega)\right],$$

and subtracting 15 from 12 yields:

$$f^+(z_1, z_2)G^{-,+}(z_1, z_2) + f^-(z_1, z_2)\overline{G}^{-,-}(z_1, z_2) = \quad (17)$$
$$\left[G^{-,+}(z_2, z_2) - \overline{G}^{+,-}(z_2, z_2)\right].$$

Based on Expression 17 we can form a double-focusing imaging condition of the scattering-type, we evaluate this considering the effect of model errors in Equations 6 to 9:

$$I_R(z_2) = \int\left[\widetilde{f}^+(z_1, z_2)\overline{\widetilde{G}}^{-,+}(z_1, z_2) + \widetilde{f}^-(z_1, z_2)\overline{\widetilde{G}}^{-,-}(z_1, z_2)\right]d\omega$$

$$= \int\left[R^{\cup}(z_2) - R^{\cap}(z_2)\right]\alpha^2(z_1, z_2)\exp\{i\omega 2\beta(z_1, z_2)\}d\omega, \quad (18)$$

where we used $\int G^{-,+}(z, z)d\omega = \int R^{\cup}(z)d\omega$, and $\int G^{+,-}(z, z)d\omega = \int R^{\cap}(z)d\omega$. Integration over frequency is equivalent to extracting the zero-time component in the time domain. Based on Expression 16 we can form a double-focusing imaging condition of the source-type, we evaluate this considering the effect of model errors in Equations 6 to 9:

$$I_S(z_2) = -\int\left[\widetilde{f}^+(z_1, z_2)\widetilde{G}^{-,-}(z_1, z_2) + \widetilde{f}^-(z_1, z_2)\overline{\widetilde{G}}^{-,+}(z_1, z_2)\right]d\omega$$

$$= \int\left[\overline{G}^{+,+}(z_2, z_2) - G^{-,-}(z, z)\right]\alpha^2(z_1, z_2)d\omega. \quad (19)$$

Imaging condition 19 extracts the virtual-source focusing strength. When we including the effect of a finite frequency source wavelet and normalized the image to the peak amplitude of the zero-phase source wavelet, the imaging condition in Equation 19 will result in the square of the amplitude error, $I_S(z_2) = \alpha^2(z_1, z_2)$. In the absence of model errors, this image will be in $I_S(z_2) = 1$.

Figure 3 contains gathers showing the evaluation of Equations 17 and 16 at each depth level, with and without model errors. Figures 4a and 4b contains the images, $I_R(z)$ and $I_S(z)$, also obtained by extracting the t=0 slice from the gathers in Figure 3.

DISCUSSION

When we neglect the inhomogeneities in the subsurface we omitted a transmission coefficient from the estimated DWGF. A factor $T_{1,2}^+ = \sqrt{1 - (R_{1,2}^{\cup})^2}$; $T_1^+ \approx 0.990$ and $T_2^+ \approx 0.994$ at the first and second interface respectively. This leads to the factor $\alpha(z(t)) = T_1^+$ for $z(t) > z(\tau_1)$, and $\alpha(z(t)) = T_1^+ T_2^+$ for $z(t) > z(\tau_2)$, where $\widetilde{\tau}_{1,2}$ are the estimated one-way travel times to the first and second interfaces respectively. This corresponds to where the dashed blue curve in Figure 4a levels out at $0.980 = 0.990^2$ and $0.967 = (0.990 \times 0.994)^2$. The dashed blue curve in Figure 4a corresponds to an image strength of $R_2^{\cup}(T_1^+)^2 \approx 0.109$ at the second interface, located at $z(\tau_2)$.

A conventional deconvolution imaging condition seeks to find a reflection response of a truncated medium by solving $G^{-,+}(z_2, z_1) = R^{\cup}(z_2)G^{+,+}(z_2, z_1)$, the image is extracted by evaluating $R^{\cup}(z)\big|_{t=0}$:

$$I_3(z) = \left[\widetilde{G}^{+,+}(z, z_1)\right]^{-1}\left[\widetilde{G}^{-,+}(z, z_1)\right]\Big|_{t=0} = \quad (20)$$
$$R^{\cup}(z, \omega)\exp\{i\omega 2\beta(z, z_1)\}\Big|_{t=0}.$$

This imaging condition is insensitive to the amplitude error. However, just as in the new imaging condition in Equation 20, the kinematic phase-error is doubled. This phase error causes our imaged reflectors to appear at the incorrect depth level.

Based on the imaging conditions in Equations 18 and 19 we define an imaging condition as $I = I_S^{-1}I_R$, the remaining phase error is equal to the phase in the deconvolution imaging condition (Equation 20), but we would avoid the instability due to deconvolution.

The amplitude error can only be inverted for the accompanying phase error if we make assumptions regarding the density of the medium. Conventional velocity analysis from seismic data inherently requires data in two or higher dimensions, to perform some sort of moveout analysis for non-zero offset recordings (Biondi, 2006). Whether MWR allows for such analysis remains to be seen.

CONCLUSIONS

Based on double focusing principles we formulated two novel imaging conditions for MWR. These yield direct information on the amplitude error in the estimate for the direct-wave GF, and indirect information on the phase error. Direct information on the phase error remains elusive.

ACKNOWLEDGMENTS
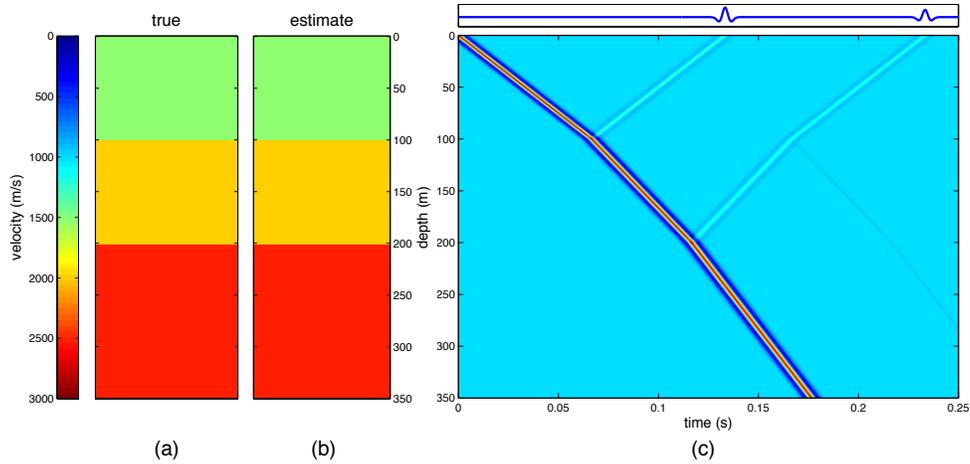
Figure 1: Surface reflection data extrapolated into the subsurface using focussing functions found by solving the Marchenko equations. a) True subsurface model governing the reflection data. b) Estimate of subsurface model governing the direct focusing function: equal to the true model. c) Extrapolated wavefield plus the original recorded reflection data trace (top panel).
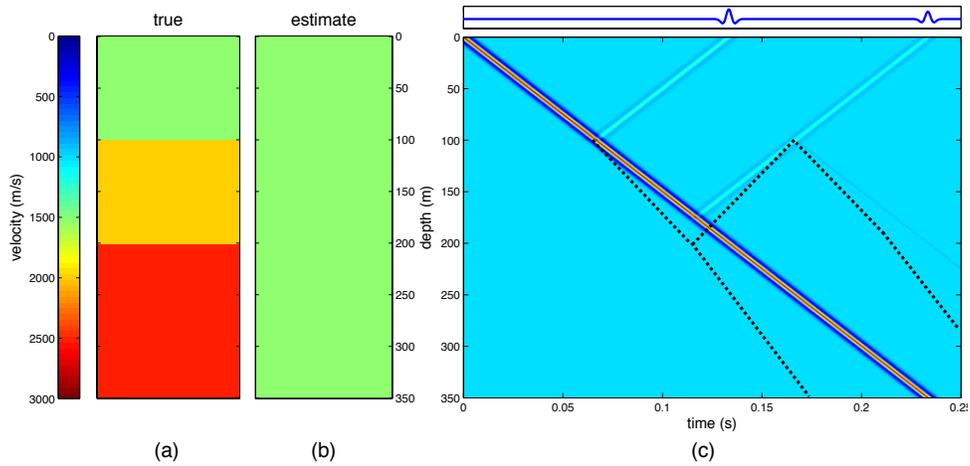
Figure 2: Surface reflection data extrapolated into the subsurface using focussing functions found by solving the Marchenko equations. a) True subsurface model governing the reflection data. b) Estimate of subsurface model governing the direct focusing function: simply a constant background velocity. c) Extrapolated wavefield plus the original recorded reflection data trace (top panel). Dotted lines indicate the location of the true wavefield in the subsurface (from Figure 1).
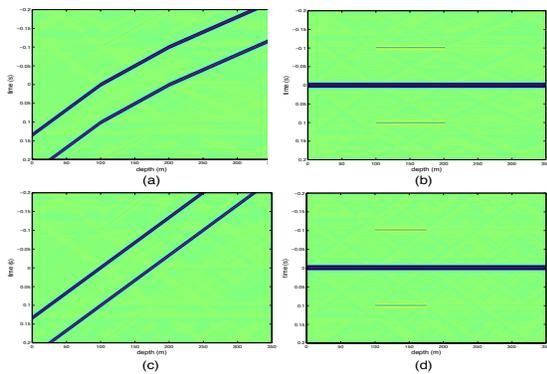
Figure 3: Double-focusing source and scattering type images as a function of time and depth. a & c) Scattering-type image in true (a) and homogeneous background (c) models. b & d) Source-type image in true (b) and homogeneous background (d) models.
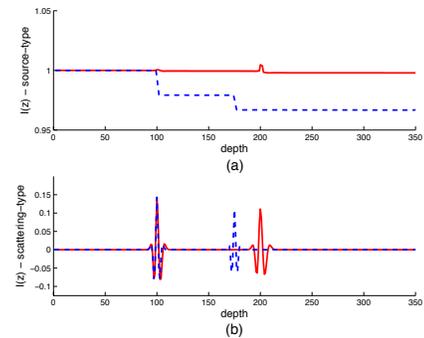
Figure 4: Double-focusing source and scattering type images as a function of depth only. Red curves are the images using the true model (Figure 1). Blue curves are the images using the model with the homogeneous background model (Figure 2).